sustainability

MDPI

Article

Settlement Behavior of Shallow Foundations in Unsaturated Soils under Rainfall

Yongmin Kim [1,*], Hyundo Park [2] and Sangseom Jeong [3]

[1] School of Civil and Environmental Engineering, Nanyang Technological University, Singapore 639798, Singapore
[2] Division of Geotechnical and Tunnel Engineering, Dohwa Engineering Co., LTD, Seoul 135518, Korea; park-0809@dohwa.co.kr or park-0809@yonsei.ac.kr
[3] Department of Civil and Environmental Engineering, Yonsei University, Seoul 03722, Korea; soj9081@yonsei.ac.kr
* Correspondence: kimkimym@ntu.edu.sg; Tel.: +65-9085-4102

Received: 3 July 2017; Accepted: 8 August 2017; Published: 11 August 2017

Abstract: Shallow foundations are often situated on unsaturated zones above the groundwater table. In this study, the influence of rainfall infiltration on the settlement behavior of shallow foundations was investigated using numerical analyses. The numerical solutions were compared with experimental data from in-situ load tests. The relative importance of rainfall intensities and groundwater table positions in inducing the additional settlement of shallow foundations was examined through a series of parametric studies. Two different groundwater table positions contributing to settlements and three assorted rainfall intensities were used in the numerical analyses. Typical soil properties of two main residual soils in Korea were incorporated into the numerical analyses. Special attention is given to the sequential analysis procedure comprised of a flow analysis and deformation analysis. Load-settlement relationships obtained from the numerical methodology in the present study were in good agreement with the field measurements. Results from the parametric studies showed that the rainfall intensity plays a significant role in the settlement behavior of shallow foundations in unsaturated soils. The changes in the settlement during rainfall were also affected by the groundwater table position near the ground surface due to changes in matric suction. In addition, higher bearing capacity in response to rainfall infiltration was observed in the soil with smaller permeability function as compared to larger permeability function.

Keywords: settlement; shallow foundation; unsaturated soil; rainfall infiltration; modulus of elasticity; sequential analysis

1. Introduction

Settlement is one of the key parameters in designing shallow foundations. The conventional design of shallow foundations is carried out by following the principles of saturated soil mechanics. However, the soils near the ground surface are usually in an unsaturated state because the groundwater table is deep. Shallow foundations are built within unsaturated zones ignoring the influence of matric suction in unsaturated soils.

A considerable number of researchers have found that the settlement of shallow foundations is significantly affected by the existence of matric suction, resulting in an increase in the shear strength of the soil [1–4]. Rahardjo et al. [5] reported that the modulus of elasticity in unsaturated soil appears to increase with increasing matric suction. Oh et al. [6] has also formulated the variation of the modulus of elasticity with respect to matric suction as a functional relationship incorporating the soil-water characteristic curve (SWCC). Nevertheless, it can be pointed out that most studies have been neglecting the influence of matric suction, resulting in an overestimation of the settlement of shallow

foundations. Despite a growing interest in the use of matric suction for assessing the settlement, very few studies have examined the transient process inducing additional settlement of shallow foundations [7–9], because of the uncertainties in boundary conditions and difficulties in determining the input parameters for constitutive equations.

This study has under taken a two-dimensional (2D) finite element (FE) analysis using the commercial software, PLAXIS 2D [10] to study the load-settlement behavior of shallow foundations in unsaturated soils under rainfall. Special attention is given to the sequential analysis procedure that is comprised of a flow and deformation analysis. The numerical methodology and analysis results were validated against field measurements. The relative importance of rainfall intensities and groundwater table positions in inducing the settlement of shallow foundations were investigated through a series of parametric studies. Two different groundwater table positions (1B and 2B below a ground surface, where B is the foundation width) contributing to settlements and three assorted rainfall intensities (10, 20, and 30 mm/h) were used in the numerical analyses. Typical soil properties of two main residual soils in Korea were incorporated into the numerical analyses. The modulus of elasticity for unsaturated soils was determined using the semi-empirical model proposed by Oh et al. [6]. In combination of finite element (FE) method, the observation gives insight to understand the influence of matric suction on the settlement behavior of shallow foundations in unsaturated soils.

2. 2D Finite Element Modelling of Unsaturated Soils

2.1. Estimation of Modulus of Elasticity for Finite Element Analysis

Settlement of shallow foundations may not be reliable because the influence of matric suction in unsaturated soils above the groundwater table cannot be incorporated in the results of in-situ load tests. This results in difficulties in estimating uniform and differential settlements of the shallow foundation in unsaturated soils. Oh et al. [6] analyzed a load-settlement behavior of model footing tests for three different sands under different matric suctions. They proposed a semi-empirical equation to estimate the modulus of elasticity for unsaturated soils with respect to matric suction using the modulus of elasticity for saturated condition, the soil-water characteristic curve (SWCC), and two fitting parameters, α and β as follows:

$$E_{i(unsat)} = E_{i(sat)}\left[1 + \alpha \frac{u_a - u_w}{p_a/101.3} S^{\beta}\right] \quad (1)$$

where $E_{i(unsat)}$ is the modulus of elasticity under unsaturated condition, $E_{i(sat)}$ is the modulus of elasticity under the saturated condition, p_a is the atmospheric pressure (i.e., 101.3 kPa), S is the degree of saturation, and α and β are the fitting parameters. The nonlinear variation of the modulus of elasticity with respect to matric suction is dependent on α and S^{β} in Equation (1). The relationship between matric suction and degree of saturation can be obtained from the SWCC. This study utilized Equation 1 with the fitting parameter values of α = 0.05 and β = 1 to estimate the modulus of elasticity for unsaturated soils in the numerical analyses.

2.2. Modelling of Matric Suction

In PLAXIS 2D software, the variation of negative pore-water pressure (i.e., matric suction) with depth can be simulated by defining an initial groundwater table position and maximum negative pore-water pressure head on the assumption that it varies hydrostatically with distance above and below the initial water table as shown in Figure 1. For instance, if the maximum negative pressure head, $H_{\max}$, is lower than the height of the unsaturated soil layer, H_{unsat} (i.e., $H_{\max} < H_{unsat}$), the negative pore-water pressure is constant up to the ground surface beyond the maximum negative pressure head. On the other hand, if the maximum negative pressure head is greater than the height of the unsaturated soil layer (i.e., $H_{\max} \geq H_{unsat}$), the negative pore-water pressure increases hydrostatically up to the ground surface.

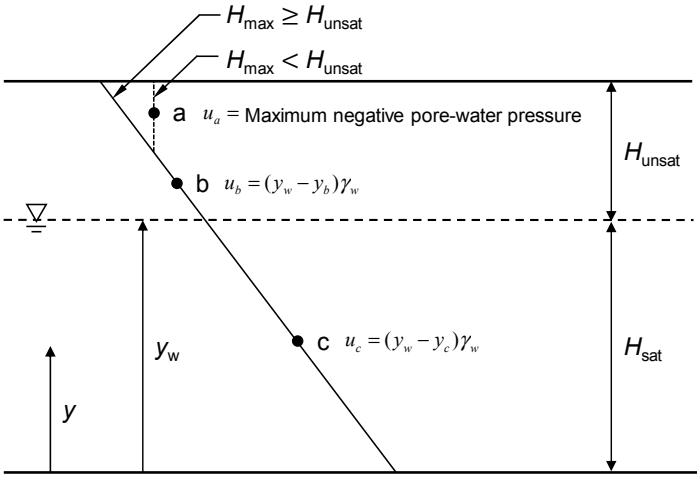

Figure 1. Modelling of matric suction using PLAXIS 2D.

2.3. Estimation of Effective Internal Friction Angle and Dilation Angle

Hossain and Yin [11] reported that the dilatancy angle of unsaturated soils increased with increase in matric suction based on their laboratory test results. Nevertheless, this cannot be used to explain the entire mechanics of dilatancy angle of unsaturated sand. The increasing of friction angle for unsaturated sands can be explained using the equation proposed by Bolton [12],

$$\phi' = \phi'_{crit} + 0.8\psi_p \tag{2}$$

where ϕ' is the effective internal friction angle, ϕ'_{crit} is the critical state internal friction angle, and ψ_p is the peak dilatancy angle given by

$$\psi_p = \begin{cases} 6.25I_R \text{ for plane-strain conditions} \\ 3.75I_R \text{ for triaxial conditions} \end{cases} \tag{3}$$

where I_R is the dilatancy index that is given by

$$I_R = I_D \left[Q + \ln\left(\frac{P_A}{100P'_p} \right) \right] - 1 \tag{4}$$

where I_D is the relative density (as a number between 0 and 1), P_A is the reference pressure (= 100 kPa), P'_p is the mean effective stress at peak strength, and Q is the intrinsic soil variable, approximately equal to 10 for silica sands [13].

Hence, ϕ'_{crit} is the friction angle of sands under the critical state (shearing occurred without any dilatancy). ϕ'_{crit} is often regarded as constant for sand under different conditions, then increasing of dilatancy angle means increasing of friction angle. Therefore, it is implemented to represent the variation of dilatancy angle with the friction angle.

3. Numerical Analysis for Simulating Field Load Tests

3.1. Site Investigation

In this study, the field test program of Texas A&M University National Geotechnical Experimentation Site [14] was chosen to investigate the response of shallow foundations subjected to vertical load in unsaturated soils. A series of field and laboratory tests were performed in order

to characterize the in-situ soil properties. Four sets of foundations were tested at the sand site (i.e., 1.0 × 1.0 m^2, 1.5 × 1.5 m^2, 2.5 × 2.5 m^2, and 3.0 × 3.0 m^2).

Figure 2 shows the typical soil profile at the load test site. The standard penetration tests (SPT) results indicated that the soil in the upper layer at a depth of 11 m was medium-dense silty sand. Fine material contents were from 2 to 8% and 5 to 30% at 3 m and 9 m depth, respectively. Below the sand layer overlain by hard clay layer until a depth of 33 m from ground level. According to the Unified Soil Classification System (USCS), the weathered soil was classified as silty sand (SM). The index soil properties based on the site investigations are summarized in Table 1.

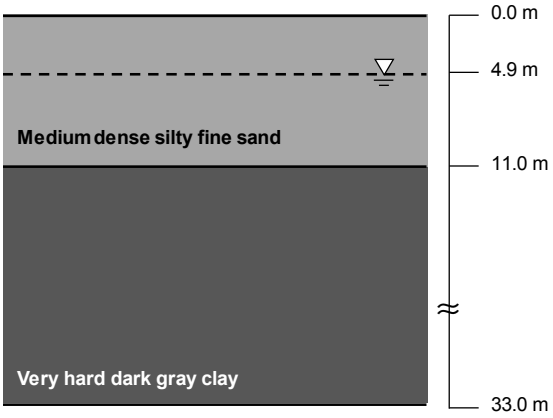

Figure 2. Typical soil profile at load test site.

Table 1. Index properties of soil at load test site [14].

Soil Property	Value
Specific gravity, G_s	2.64
Water content, w (%)	5.0
Void ratio, e	0.78
Unity weight, γ (kN/m^3)	17.75
USCS [1]	SM

[1] Unified Soil Classification System.

3.2. Finite Element Modeling

Numerical analysis was carried out to simulate the load-settlement behavior of four different size of plate load tests for unsaturated conditions using the commercial software, PLAXIS 2D [10]. A drained condition was considered during the load-settlement simulation. The model boundaries extended to 18 m in depth and 30 m in width. The vertical boundaries were restrained in the horizontal direction, while it was free in the vertical direction. The bottom boundary was restrained in both vertical and horizontal directions (Figure 3).

The sand and foundation were modelled using triangular elements with 15 nodes. The sand was modelled as an elasto-plastic material using the Mohr–Coulomb model considering the dilatancy effect of the sand. The shear strength parameters (c', ϕ'), dilation angle (ψ) of the sands for unsaturated conditions were incorporated into the Mohr–Coulomb model. In particular, the modulus of elasticity ($E_{i(unsat)}$) of unsaturated soil was estimated from Equation 1 with fitting parameters (α = 0.05 and β = 1.0). The calculated $E_{i(unsat)}$ was manually implemented by PLAXIS 2D [10]. The footing was modelled as a linear-elastic material. The material properties of unsaturated soils and foundation used in the numerical analysis are presented in Table 2.

Distributed load was applied vertically over the footing without the eccentricity. An initial stress was developed by deactivating the foundation. It was assumed that the self-weight of the

foundation was added to the distributed load. Two staged constructions were carried out. In the first staged construction, the foundation was placed and in the second staged construction, the loading was activated. Finally, an incremental multiplier was applied for the vertical load to failure. The simulations of different size of shallow foundations were performed with plane dimensions 1.0×1.0 m^2, 1.5×1.5 m^2, and 2.5×2.5 m^2, and 3.0×3.0 m^2.

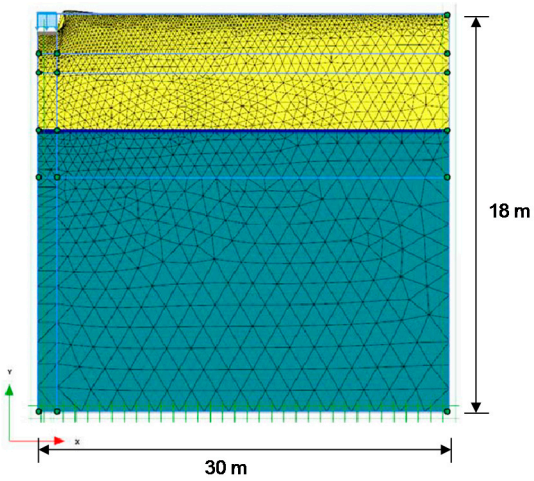

Figure 3. Finite element model for simulating field load test.

Table 2. Material properties of unsaturated soil and foundation used in numerical analysis.

Soil Property	Value
Effective internal friction angle, ϕ' (deg)	35
Effective cohesion, c' (kPa)	1
Dilation angle, ψ (deg)	26
Poisson's Ratio, ν	0.3
Modulus of elasticity of soil, $E_{i(unsat)}$ (MPa)	45
Modulus of elasticity of footing, E_f (MPa)	30,000

3.3. Comparison with Field Measurements

Figure 4 shows the predicted and measured load-settlement responses for different sizes of foundations. As shown in the figure, the results of the numerical analyses were very close to those obtained from the field load tests of 1.0×1.0 m^2, 1.5×1.5 m^2, 2.5×2.5 m^2, and 3.0×3.0 m^2 foundations. A stiffer load-settlement response was observed in the field load test of 1.5×1.5 m^2 foundation as compared to the result of the numerical analysis. This indicates the limitation of the numerical analysis method used in this study. The settlement behavior of shallow foundations in the unsaturated soil, which depends on types of soil, degree of saturation, and anisotropy, cannot be simply simulated through the numerical method in an idealized condition. Although the numerical analysis method presented in this study has such limitations, the general trend of the measured settlement behavior of the foundations is fairly well predicted.

The case of the 3.0×3.0 m^2 foundation exhibits higher settlement than the relatively lower dimensions as shown in Figure 4. However, Briaud [15] suggested that the size effect can be eliminated by plotting the load-normalized settlement (i.e., δ/B) curves. Similar trends are reported in the literature [16]. According to the report published by Federal Highway Administration (FHWA) [17], this behavior can be explained using triaxial test analogy. If triaxial tests are conducted for identical sand samples under the same confining pressure where the top platens are different sizes of footings, the stress versus strain behaviors for the samples are unique regardless of the diameter of the samples. In addition, Consoli et al. [18] reported that the uniqueness of the normalized curves can be observed

at sites where the soils are homogeneous and isotropic in nature. Thus, the size effect can be ignored in the numerical analyses and results.

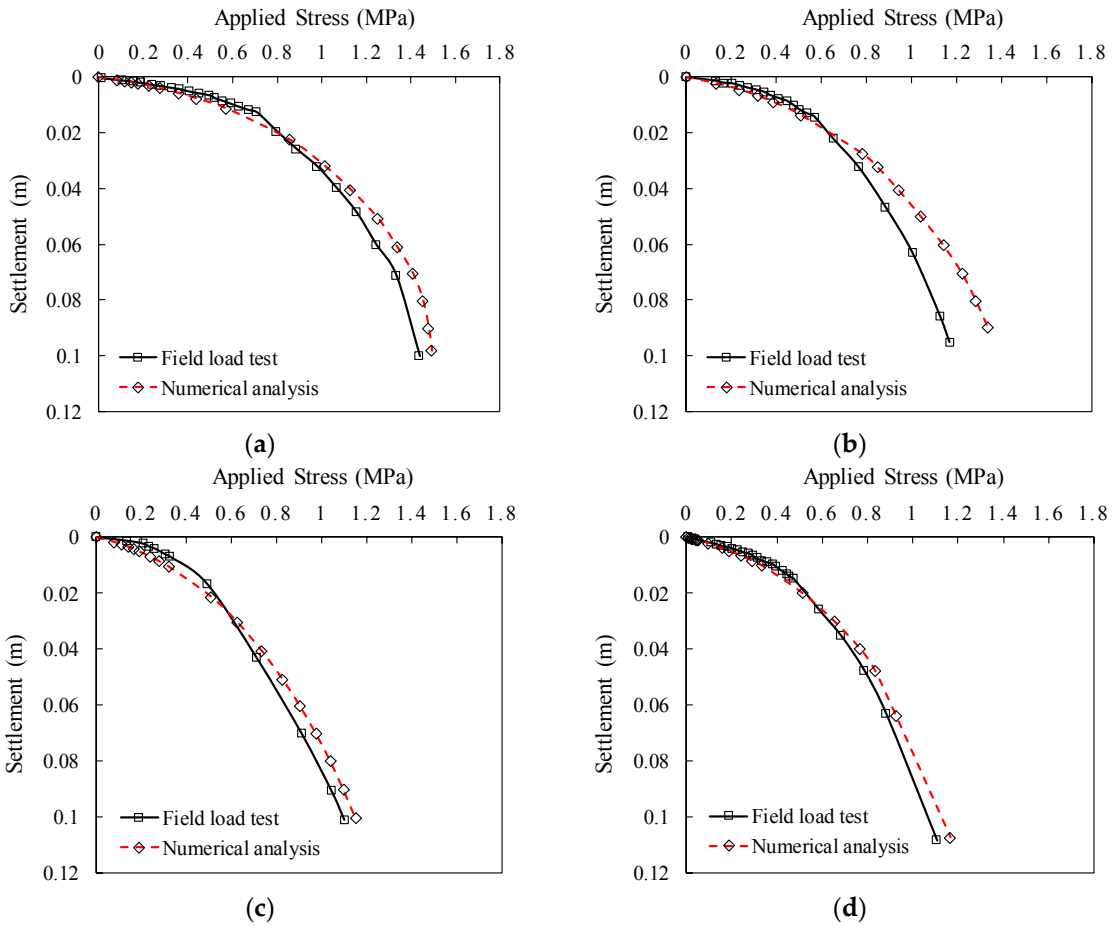

Figure 4. Comparison of load-settlement responses between numerical and measured results: (**a**) 1.0 × 1.0 m^2 foundation; (**b**) 1.5 × 1.5 m^2 foundation; (**c**) 2.5 × 2.5 m^2 foundation; (**d**) 3.0 × 3.0 m^2 foundation.

3.4. Load-Settlement Behavior with Respect to Initial Matric Suction

The soil below the foundation typically experience wetting-drying cycles due to the reasons mostly associated with climatic conditions (i.e., rain infiltration or evaporation). Hence, it is also important to estimate the variation of load-settlement behavior with respect to matric suction. To simulate the load-settlement behavior of the in-situ shallow foundation, a 2.5 × 2.5 m^2 foundation was chosen. The influence of wetting-drying cycles and external loads on the SWCC is not taken into account in the analysis due to the limited information.

The variation of the load-settlement behavior with respect to matric suction from the numerical analysis is shown in Figure 5. Figure 6 shows the variation of the settlement under a constant stress of 0.315 MPa and the various stresses that cause the 25 mm settlement with different matric suctions, respectively. Figure 6a shows that the settlement for the saturated condition under 0.315 MPa is 25 mm and the settlement will drop due to the existence of matric suction. The settlement tends to recover after matric suction exceeds 6 kPa. Similarly, Figure 6b shows that the settlement of 25 mm was induced at 1.7 times less stress as the soil becomes saturated conditions (i.e., from 10 to 0 kPa). This result could be attributed to the high modulus of elasticity as matric suction increases.

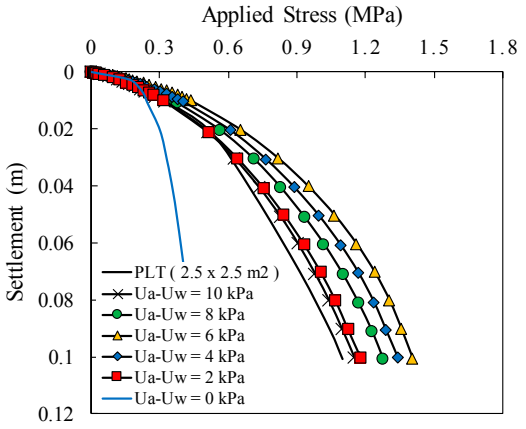

Figure 5. Variations in load-settlement response of shallow foundation with various matric suction.

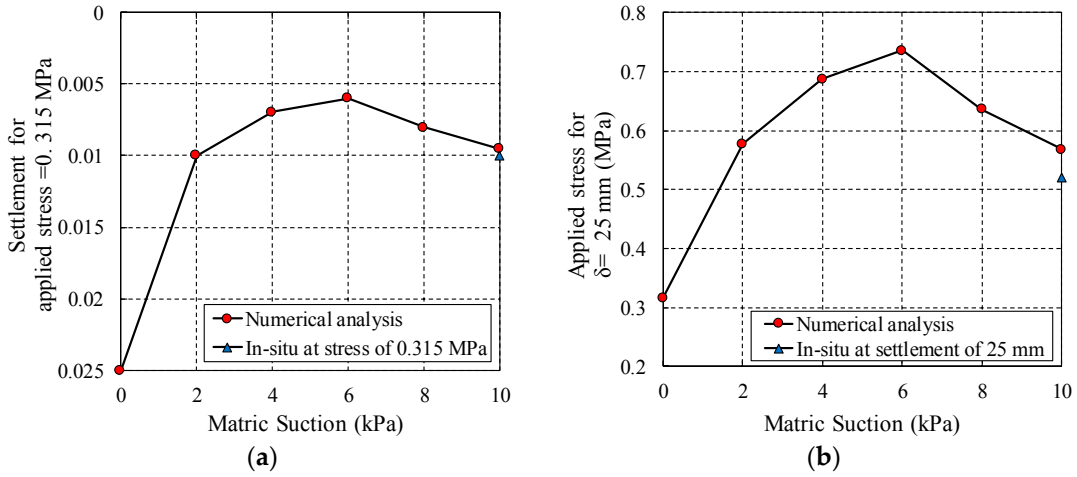

Figure 6. Variations in (**a**) the settlement under the applied stress of 0.315 MPa; (**b**) the applied stress causing the settlement of 25 mm.

4. Effect of Rainfall Infiltration on Settlement Behavior of Shallow Foundation

The sequential analysis was conducted to highlight the effect of rainfall infiltration on the settlement of shallow foundations under different hydraulic boundary conditions (i.e., rainfall and groundwater table conditions). The settlement is assessed through the soil conditions, rainfall intensities, rainfall durations, and different groundwater table positions.

4.1. Model and Parameters

A two-dimensional finite element model using PLAXIS 2D [10] was developed to investigate the effects of rainfall infiltration on the settlement behavior of shallow foundations. Figure 7 shows the initial and boundary conditions for a simple circular foundation to simulate the matric suction distribution under rainfall. A 5.0 × 5.0 m^2 foundation was resting on the unsaturated soil of 30 m height followed by 55 m of length.

Most dominant types of soils in Korea (i.e., SM and SP) were selected to perform parametric studies [19]. It is worthwhile to note that the symbols Type A and Type B will be used to denote these two soils. The groundwater table position was assumed to be either 1 or 2 B below the ground surface, where B is the foundation width. Poulos and Davis [20] suggested that when a load is applied to a shallow foundation, the stress transferred to the ground due to the load is predominant in the 0 to

1.5 B depth region. The stress increment below a square foundation at a depth deeper than 1.5 B is less 15% of the applied stress at the ground surface.

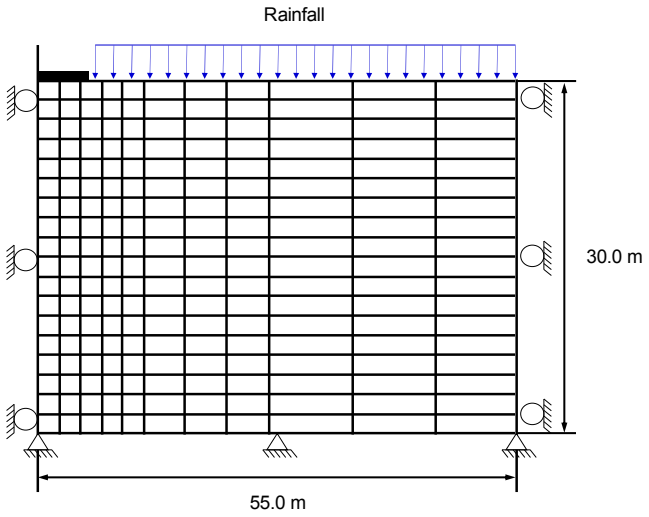

Figure 7. 2D finite element model and boundary condition used in parametric study.

The wetting soil-water characteristic curves (SWCCs) were inferred from the van Genuchten's equation [21] as shown in Figure 8. The mechanical and hydraulic properties of both types of soils used in the numerical analysis are summarized in Tables 3 and 4, respectively. The influence of hysteresis between drying and wetting process is not taken into account in the analysis. Boundary conditions were applied to the foundation model for the transient seepage analysis. The flux boundary, q, equal to the desired rainfall intensity (e.g., 10 mm/h, 20 mm/h and 30 mm/h) and duration (1 h to 96 h) were applied to the top surface of the ground. The saturated permeability of Type A (4.67×10^{-5} m/s) is far greater than the rainfall intensity of 10 mm/h (5.12×10^{-6} m/s). The saturated permeability of Type B (5.12×10^{-6} m/s) is almost equal to the rainfall intensity of 10 mm/h (5.12×10^{-6} m/s). The impermeable boundary condition on the right, left and bottom sides of the soil was applied to simulate no-flow zones. The finite element model of the whole foundation was discretized with a mesh size of approximately 0.75 m to obtain accurate results. The sequential analysis procedure using PLAXIS 2D [10] is presented in Figure 9 and the analysis cases with respect to rainfall intensities and groundwater table positions are summarized in Table 5.

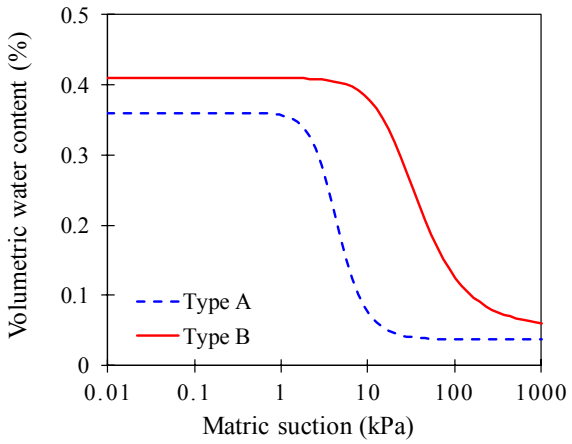

Figure 8. Soil-water characteristic curves for typical two types of soils.

Table 3. Mechanical properties of two types of soils used in parametric study.

Soil property	Type A	Type B
Specific gravity, G_s	2.64	2.72
Max. dry unit weight, $\gamma_{d,\max}$ (kN/m^3)	17.1	17.5
Min. dry unit weight, $\gamma_{d,\min}$ (kN/m^3)	13.3	13.5
Cohesion, c (kPa)	1.0	10.7
Internal friction angle, ϕ (deg)	22.8	35.0
Saturated Elastic Modulus, $E_{i(sat)}$ (MPa)	1.5	2.5
Possion's ratio, ν	0.3	0.3

Table 4. Hydraulic properties of two types of soils used in parametric study.

Soil Property	Type A	Type B
Fitting parameter for SWCC, α (1/kPa)	0.27	0.042
Fitting parameter for SWCC, n	3.10	2.06
Saturated volumetric water content, θ_s	0.36	0.41
Residual volumetric water content, θ_r	0.037	0.054
Saturated permeability, k_s (m/s)	4.67×10^{-5}	5.12×10^{-6}

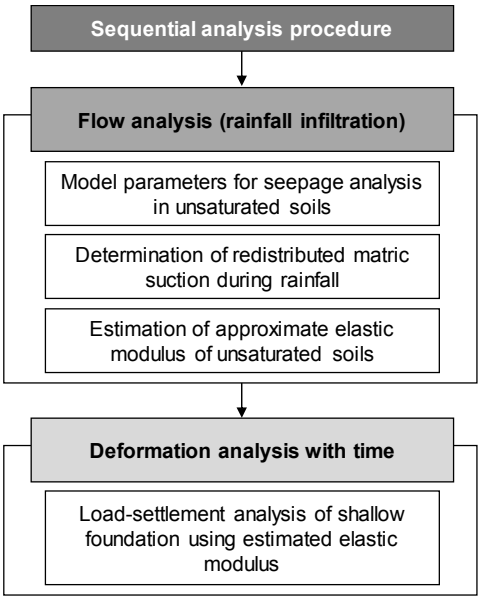

Figure 9. Sequential analysis procedure based on PLAXIS 2D analyses.

Table 5. Summary of combination of factors affecting settlement used in parametric study.

Soil Types	Footing Size	Groundwater Table Position	Rainfall Intensity	Rainfall Duration
Type A Type B	5 × 5 m	1B 2B	10 mm/h 20 mm/h 30 mm/h	1 h 3 h 6 h 12 h 24 h 48 h 96 h

4.2. Load-Settlement Responses under Rainfall

Figure 10 shows the load-settlement curves of the 5 × 5 m^2 foundation subjected to rainfall intensity of 10 mm/h with the groundwater table 1B below. The figure shows that the initial slope of load-settlement curves decreases continuously with an increase in the rainfall duration, which represents the decrease in the bearing capacity of shallow foundations. After 48 hours, the bearing capacity of shallow foundations in both Type A and B soils rapidly drop due to rainfall infiltration. It is attributed to the settlement taking place essentially during the first two days, then accelerates until the soil reaches a full saturation. It is also found from Figure 10 that the bearing capacity of a shallow foundation in Type B soil exhibits higher bearing capacity as compared to Type A soil. This behavior indicates that rainfall infiltration into the unsaturated soil, which is affected by permeability functions, has significant effect on the load-settlement response curve as matric suction decreases. It can be said that the additional settlement is induced by rainfall infiltration and loss of matric suction. Figure 11 shows matric suction distributions in two types of the soil. Decreases in matric suction in Type A soil are more significant than in Type B due to the low permeability of the soil, resulting in the slow infiltration process of rainwater into greater depths. Note that these matric suction values at different time steps are used in the deformation analysis routine to evaluate the modulus of elasticity and the corresponding settlements.

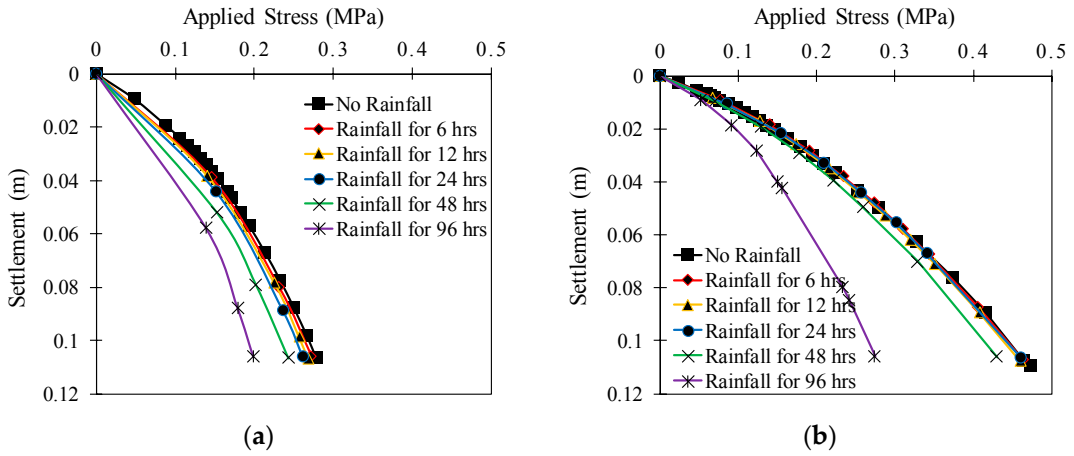

Figure 10. Load-settlement curves of 5 × 5 m^2 foundation (rainfall intensity of 10 mm/h, groundwater table 1B below): (**a**) Type A; (**b**) Type B.

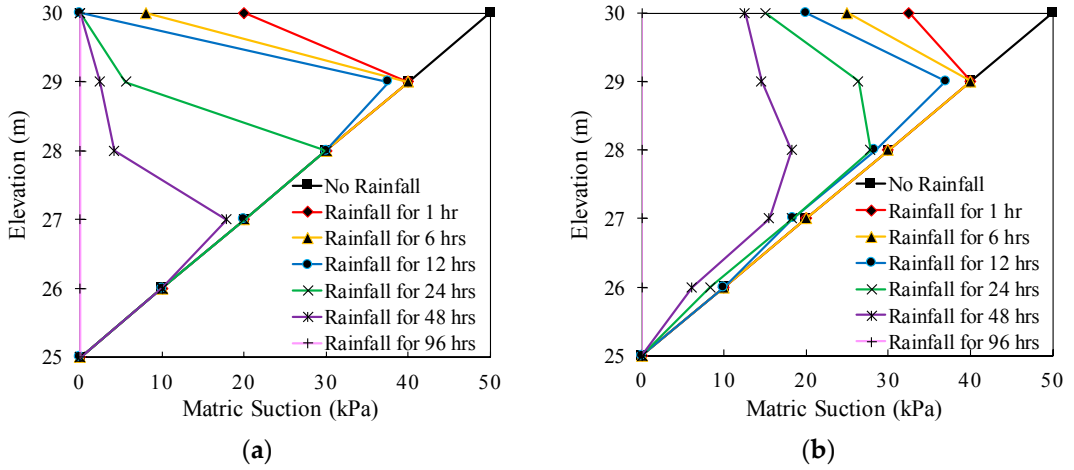

Figure 11. Matric suction distribution of 5 × 5 m^2 foundation (rainfall intensity of 10 mm/h, groundwater table 1B below): (**a**) Type A; (**b**) Type B.

4.3. Settlement of Shallow Foundation with Time

Variations in the settlement of shallow foundations with respect to rainfall intensities (10, 20 and 30 mm/h) and groundwater table positions (1B and 2B) for different soil types (Type A and Type B) are shown in Figures 12 and 13. The plots of variations in settlements versus time under different rainfall intensities show that rainfall infiltration induces the settlement increase due to the loss of matric suction above the groundwater table. As the rainfall intensity escalates, the settlement in Type A soil increases gradually and the rate of additional settlement tends to be influenced by rainfall intensity as shown in Figures 12a and 13a. On the contrary, the settlement in Type B soil increases rapidly and reaches almost a constant settlement when the rainfall intensity exceeds 10 mm/h as shown in Figures 12b and 13b. This could be attributed to the rate of rainfall infiltration into the soil, which leads to different elastic modulus of unsaturated soils due to different matric suction distributions. It means that Type B soil remains unsaturated, while Type A soil has become saturated during rainfall. It is also observed that the groundwater table near the top surface of soil yields an additional settlement as compare to the deeper groundwater table as shown in Figures 12 and 13. The settlement of shallow foundations obtained from numerical analyses with various hydraulic conditions are summarized in Table 6.

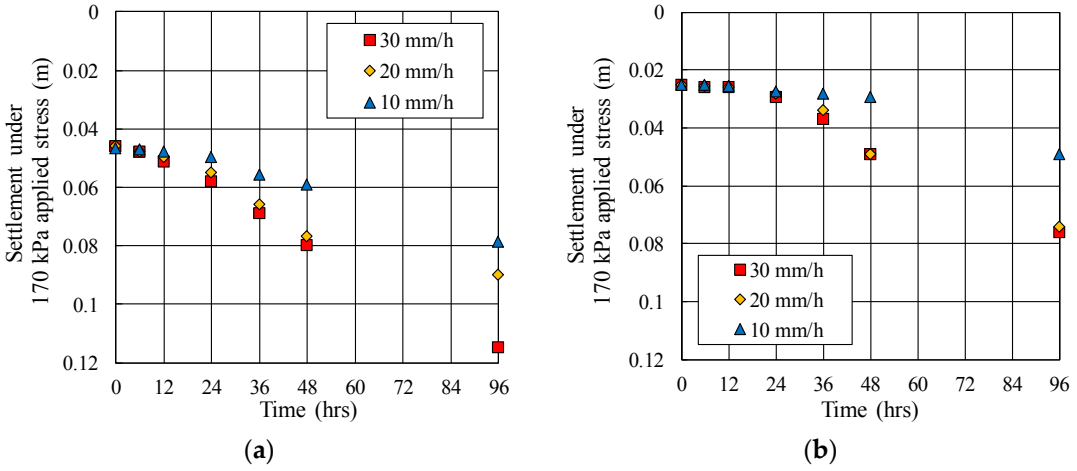

Figure 12. Variations in the settlement of shallow foundation under 170 kPa applied stress for groundwater table 1B below: (**a**) Type A; (**b**) Type B.

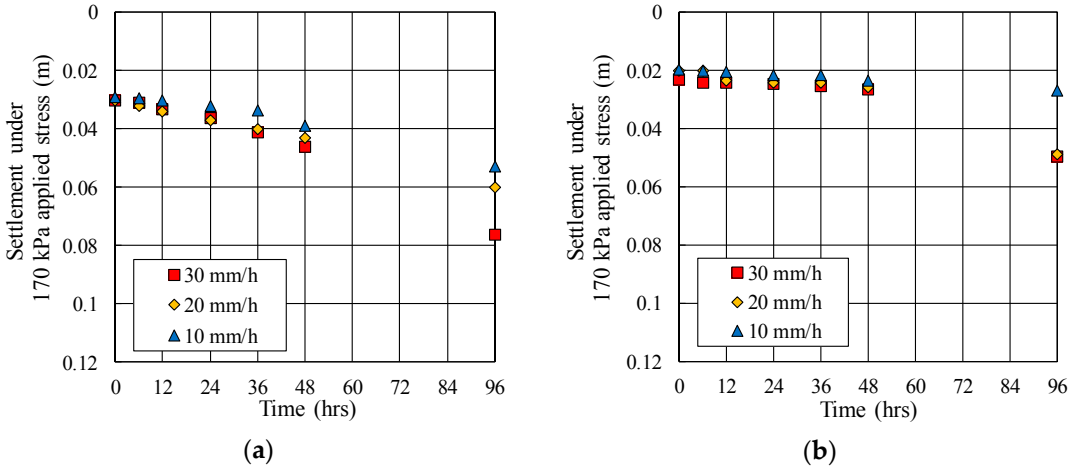

Figure 13. Variations in the settlement of shallow foundation under 170 kPa applied stress for groundwater table 2B below: (**a**) Type A; (**b**) Type B.

Table 6. Summary of settlements for shallow foundation with various hydraulic conditions.

	Settlement in Type A Soil (mm)			Settlement in Type B Soil (mm)		
	10 mm/h	20 mm/h	30 mm/h	10 mm/h	20 mm/h	30 mm/h
Time	**Groundwater table 1B Below**					
0	47.0	46.0	46.0	25.1	25.1	25.1
6	47.3	48.0	48.0	25.3	25.5	25.9
12	48.0	50.0	51.5	25.6	25.8	26.0
24	50.0	55.0	58.0	27.5	28.3	29.2
36	56.0	66.0	69.0	28.4	33.9	36.9
48	59.1	77.0	80.0	29.5	49.0	49.0
96	78.9	90.0	115.0	49.2	74.0	76.0
Time	**Groundwater table 2B Below**					
0	29.0	30.0	30.0	19.5	19.9	23.2
6	29.3	31.9	31.0	20.0	20.0	24.0
12	30.0	34.0	33.0	20.2	23.6	24.2
24	31.9	37.0	36.0	21.5	23.9	24.6
36	33.6	40.0	41.0	21.6	24.3	25.2
48	39.0	43.0	46.0	23.5	25.5	26.5
96	52.5	60.0	76.0	26.7	48.6	49.5

5. Conclusions

The main objective of this study is to numerically investigate the settlement behavior of shallow foundations subjected to rainfall infiltration. For this work, the sequential finite element modeling has been presented and discussed by taking into account the modulus of elasticity of unsaturated soils. The simulation techniques and analysis results were favorably validated in the field load tests in terms of load-settlement curves on the various size of foundations. In addition, to examine the influencing factor of the settlement behavior, a series of parametric studies were performed. Based on the findings of this study, the following conclusions can be drawn:

- By taking into account the influence of matric suction in unsaturated soils, a reasonably good agreement of load-settlement responses is obtained between the numerical analysis results and field load test results for four different size of shallow foundations. The sequential analysis procedure for deformable unsaturated soils can approximate the settlement of shallow foundations with time.
- Initial matric suction of unsaturated soils exhibits obvious strengthening effects for the bearing capacity of shallow foundations with decreasing the settlement due to the high modulus of elasticity as matric suction increases. In addition, rainfall intensity plays a significant role in determining the settlement of shallow foundations in unsaturated soils. It can be said that the additional settlement is caused by rainfall infiltration and loss of matric suction.
- The change in settlements during rainfall is significantly affected by the groundwater table position near the ground surface due to changes in matric suction. In addition, higher bearing capacity in response to rainfall infiltration is observed for the soil with smaller permeability function as compared to larger permeability function.
- Therefore, the numerical simulations from the methodology presented in this study provide an initial understanding of the stability of shallow foundations for transient conditions leading to additional settlements caused by rainfall infiltration.

Acknowledgments: The authors acknowledge support in this research from the National Research Foundation of Korea (NRF) (Grant No. 2011- 0030040).

Author Contributions: All authors significantly contributed to the research. Sangseom Jeong designed this research. Yongmin Kim and Hyundo Park collected and analyzed data. Yongmin Kim wrote the paper.

Conflicts of Interest: The authors declare no conflicts of interest.

References

1. Rojas, J.C.; Salinas, L.M.; Sejas, C. Plate-load tests on an unsaturated lean clay. In *Experimental Unsaturated Soil Mechanics*; Springer: Berlin/Heidelberg, Germany, 2007; pp. 445–452.
2. Vanapalli, S.K.; Mohamed, F.M. Bearing capacity of model footings in unsaturated soils. In *Experimental Unsaturated Soil Mechanics*; Springer: Berlin/Heidelberg, Germany, 2007; pp. 483–493.
3. Jeong, S.; Kim, J.; Lee, K. Effect of clay content on well-graded sands due to infiltration. *Eng. Geol.* **2008**, *102*, 74–81. [CrossRef]
4. Kim, Y.; Jeong, S.; Kim, J. Coupled infiltration model of unsaturated porous media for steady rainfall. *Soils. Found.* **2016**, *56*, 1073–1083. [CrossRef]
5. Rahardjo, H.; Melinda, F.; Leong, E.C.; Rezaur, R.B. Stiffness of a compacted residual soil. *Eng. Geol.* **2011**, *120*, 60–67. [CrossRef]
6. Oh, W.T.; Vanapalli, S.K.; Puppala, A.J. Semi-empirical model for the prediction of modulus of elasticity for unsaturated soils. *Can. Geotech. J.* **2009**, *46*, 903–914. [CrossRef]
7. Oh, W.T.; Vanapalli, S.K. Modelling the applied vertical stress and settlement relationship of shallow foundations in saturated and unsaturated sands. *Can. Geotech. J.* **2011**, *48*, 425–438. [CrossRef]
8. Mohamed, F.M.S. Bearing Capacity and Settlement Behaviour of Footings Subjected to Static and seismic Loading Conditions in Unsaturated Sandy Soils. Ph.D. Thesis, University of Ottawa, Ottawa, ON, Canada, 2014.
9. Park, H.D. Rainfall induced load-settlement behavior of shallow foundations on unsaturated soil. Ph.D. Thesis, Yonsei University, Seoul, Korea, 2017.
10. PLAXIS 2D. *PLAXIS 2D User Manual, Version 2012*; Brinkgreve, R.B., Swolfs, W.M., Eds.; PLAXIS Inc.: AN Delft, The Netherlands, 2012.
11. Hossain, M.A.; Yin, J.H. Shear strength and dilative characteristics of an unsaturated compacted completely decomposed granite soil. *Can. Geotech. J.* **2010**, *47*, 1112–1126. [CrossRef]
12. Bolton, M.D. The strength and dilatancy of sands. *Géotechnique* **1986**, *36*, 65–78. [CrossRef]
13. Lee, J.; Salgado, R. Estimation of footing settlement in sand. *Int. J. Geomech.* **2002**, *2*, 1–28. [CrossRef]
14. Briaud, J.L.; Gibbens, R. Behavior of five large spread footings in sand. *J. Geotech. Geoenviron.* **1999**, *125*, 787–796. [CrossRef]
15. Briaud, J.L. Spread footings in sand: Load settlement curve approach. *J. Geotech. Geoenviron. Eng.* **2007**, *133*, 905–920. [CrossRef]
16. Palmer, L.A. Field loading tests for the evaluation of the wheel load capacities of airport pavements. In *ASTM STP 79*; ASTM: Philadelphia, PA, USA, 1947; pp. 9–30.
17. Briaud, J.L.; Gibbens, R. *Large Scale Load Tests and Data Base of Spread Footings on Sand*; Technical Report, FHWA–RD–068; US Department of Transportation Federal Highway Administration: Washington, DC, USA, 1997.
18. Consoli, N.C.; Schnaid, F.; Milititsky, J. Interpretation of plate load tests on residual soil site. *J. Geotech. Geoenviron. Eng.* **1998**, *124*, 857–867. [CrossRef]
19. Kim, Y.; Jeong, S. Modelling of shallow landslides in an unsaturated soil slope using a coupled model. *Geome. Eng. Int. J.* **2017**, *13*, 1–18.
20. Poulos, H.D.; Davis, E.H. *Elastic Solutions for Soil and Rock Mechanics*; Wiley: New York, NY, USA, 1974.
21. Van Genuchten, M.T. A closed-form equation for predicting the hydraulic conductivity of unsaturated soils. *Soil Sci. Soc. Am. J.* **1980**, *44*, 892–898. [CrossRef]